DEUTSCHES ELEKTRONEN-SYNCHROTRON **DESY**

DESY 87-057
June 1987



# SIMULATION OF HADRONIC SHOWERS WITH MONTE CARLO CODES: COMPARISON WITH DATA AND FIRST APPLICATION TO THE DESIGN OF THE HERA BEAM DUMP

by

F. Ebeling

*II. Institut f. Experimentalphysik, Universität Hamburg*

R. Fohrmann, U. Otterpohl

*Deutsches Elektronen-Synchrotron DESY, Hamburg*

H.-J. Möhring

*Karl-Marx-Universität, Sektion Physik, Leipzig*

ISSN 0418-9833

NOTKESTRASSE 85 · 2 HAMBURG 52

To be sure that your preprints are promptly included in the
HIGH ENERGY PHYSICS INDEX ,
send them to the following address ( if possible by air mail ) :

DESY
Bibliothek
Notkestrasse 85
2 Hamburg 52
Germany

DESY 87-057
June 1987

ISSN 0418-9833

# Simulation of Hadronic Showers with Monte Carlo Codes: Comparison with Data and First Applications to the Design of the HERA Beam Dump

F. EBELING

*II. Institut für Experimentalphysik, Universität Hamburg*

R. FOHRMANN , U. OTTERPOHL

*Deutsches Elektronen-Synchrotron DESY, Hamburg*

H.-J. MÖHRING

*Karl-Marx-Universität, Sektion Physik, Leipzig*

ABSTRACT. Three different Monte Carlo codes—GHEISHA, FLUKA82, and CASIM—have been used to simulate hadronic shower cascades in matter. The results of the longitudinal and lateral shower developments obtained by these simulations have been compared with data to estimate the systematic uncertainties of the Monte Carlo results. The codes have been applied to materials and geometries typical for the HERA proton ring.



## 1. Introduction

With the increasing energy of the planned and approved hadron accelerators, shielding considerations become more and more important. To optimize for instance the layout of machine components like beam abort systems or for the design of fixed target stations, the energy deposition resulting from the development of hadronic showers is required to be known with reasonably small statistical and systematic errors.
Monte Carlo simulations of shower cascades have been proven to be useful tools in estimating energy depositions as well as induced radioactivities and related processes like target heating. There are several Monte Carlo codes available, describing the development of hadron-induced showers [1]. Originally these codes were developed to meet different physical requirements. Some were written to study in detail the response of detectors, others for shielding considerations like particle punch-through, lateral shielding, or target heating. Therefore the programs may differ in the underlying mathematical methods as well as in the approximations applied to the physical processes. As these differences strongly affect the computing time, it is important to study their influence on the reliability of the results and the efficiency of actual calculations for given problems.
A better understanding of the systematic uncertainties of Monte Carlo simulations derived from a comparison of different codes is very important for the design of hadron calorimeters in high-energy experiments also.
In this paper we consider the performance of the three Monte Carlo codes GHEISHA [2], FLUKA82 [3], and CASIM [4], having in mind their application to the design of the beam abort system for the HERA proton ring. In Chapter 2 we briefly characterize these three codes. A comparison of the results for the longitudinal and lateral shower developments with data is given in Chapter 3. In Chapter 4 we finally report on first applications to the HERA beam dump, ending with a summarizing discussion of our results.

## 2. Characteristics of the Monte Carlo codes

The GHEISHA code was written for detector simulation and calorimetry of hadron-induced showers in cylindrical or cartesian geometries and with different materials. The program simulates the three-dimensional development of hadronic and electromagnetic cascades. The electron-photon showers are described by the EGS code [5].
All tracks are treated in detail. The treatment of high-energy interactions, nuclear excitation, Fermi motion and the generation of secondary particles is based very strongly on experimental results. Whenever data from high-energy experiments are available, they are used for the description of the shower development. The code has been optimized and tested for sampling calorimeters of different types.
Results from GHEISHA have been compared with data for incident charged pions, kaons, protons, photons, and electrons in the momentum range from 1 GeV/c up to 400 GeV/c, as well as for assemblies of particles as it happens in quark-jets. The very complex and detailed treatment of the processes leading to hadronic and electromagnetic showers allows cutoff-energies of 30 MeV or even smaller.

The hadron-cascade code FLUKA82 was developed for shielding considerations concerning high-energy proton machines [6]. It can be run in flexible geometries with different materials. The following features of the code are most important for our applications: Available event

generators [7] are able to treat all stable hadrons as incident as well as generated particles and are fairly well tested over a wide energy range up to $p\bar{p}$ -collider energies [8].
Electromagnetic showers, coupled to each hadron-cascade via the decay of neutral pions into two photons, are treated in an average way. The photon energy is deposited at a user-defined number of points, sampled from longitudinal and lateral energy-distributions. These curves have been obtained from data as well as from results of the electromagnetic shower code EGS [5].
Below a user-defined cutoff (lowest value 50 MeV) particles are assumed to be stopped in the material. Their energy is treated in the same way as the nuclear excitation energy in inelastic collisions: one third is deposited locally (simulating charged fragments, protons etc.) and two thirds isotropically around the stopping point with the mean free path of low-energy (50 MeV) neutrons.

The CASIM Monte Carlo code is aimed at studying the average development of hadronic cascade showers in cylindrical geometries. The code computes star densities (i.e., nuclear interaction densities) and energy densities deposited by the cascade. The program does not study the transport of low-energy particles ($\leq$ 0.1 GeV/c). The description of the nuclear excitation energy and nucleons emerging from intranuclear cascade processes is similar to the one used in FLUKA82.
To increase the efficiency of the code, weighting techniques are used in the simulation of particle production and energy deposition; only one particle from each inelastic interaction is traced. The particle production model used in CASIM, based on the Hagedorn-Ranft model [9], is a limited set of a few distributions. The particles considered in the calculation are protons, neutrons, and charged pions.
The description of the electromagnetic cascade induced by the decay of neutral pions into two photons is basically the same as the one used in another Monte Carlo code, AEGIS [1], which also applies weighting techniques. Due to these weighting techniques the execution time grows only logarithmically with increasing energy. In contrast, programs like GHEISHA and FLUKA82, which trace every particle, require execution times increasing almost proportionally with energy.

## 3. Comparison of Monte Carlo calculations with data

Most data on the development of showers induced by high-energy hadrons are obtained from experiments with sampling calorimeters. In our examples the active media are x-ray films or plastic scintillators. First we consider the development of 300 GeV proton showers in an iron and a lead calorimeter respectively. In the corresponding experiment [10] the three-dimensional energy densities were measured over a range of five decades by using x-ray film stacks of different sensitivities in combination with a variable beam intensity. To economize the required CPU-time for the Monte Carlo calculations by means of CASIM, FLUKA82, and GHEISHA, the shower development has been simulated in homogeneous absorbers (length 100 cm, radius 15 cm) assuming a proportionality between the energy deposition in the absorber and the response in the active medii of the experimental set-ups. (A further discussion of this assumption is given below.)
The data, originally given in arbitrary units, have been renormalized by eye to fit the Monte Carlo results (given in GeV/cm$^3$) for the shower contour at $r$ = 1 cm in iron without changing the relative magnitude of the data for different radii and materials.



The resulting curves for the iron calorimeter, shown in Fig. 1a, are generally in reasonable agreement with GHEISHA and FLUKA82. At the largest radius FLUKA82 systematically overestimates the energy density. The shower curves obtained from CASIM underestimate the energy deposition for depths up to about 50 cm by a factor of 2 to 5.
In the case of the lead calorimeter all Monte Carlo calculations show systematic deviations from the data as seen from Fig. 1b. Particularly with increasing lateral distance from the beam axis neither the position of the shower maximum nor the longitudinal attenuation can be described by the models. As in the case of the iron calorimeter the results from CASIM differ with increasing lateral distance up to a factor of 5 from both the data and the other two codes.
CASIM needs 0.14 seconds execution time on an IBM 3084 per particle incident on the iron calorimeter. Under identical beam and target conditions it is 33 times faster than FLUKA82, which is itself a factor of 25 faster than GHEISHA.

The energy dependence of the longitudinal and lateral development of pion-induced showers in an iron-scintillator calorimeter is studied in Ref. [11]. The calorimeter was built of iron plates of different thickness interspaced by 0.7 cm of scintillator; the iron plates were arranged in a periodic 6–3–6 cm structure. To guarantee a complete shower containment the trigger conditions required a longitudinal position of the shower origin in the first two iron plates. This was achieved by defining the shower vertex by an energy release larger than a few equivalent particles in the first two subsequent readout planes. To simulate these experimental conditions in our Monte Carlo studies, an energy deposition of at least 5 MeV in each of the first two readout planes was required, which corresponds to 4.2 equivalent particles.
In Fig. 2 the average longitudinal energy depositions in the readout planes obtained by GHEISHA are compared for two different situations: In model 1 the readout planes were simulated by 7 mm of scintillator material as in the experimental set-up (full-line histogram) and in model 2 by 1 mm of iron (dashed-line histogram). From these results, demonstrating the appoximate proportionality of both curves and thereby justifying the use of homogeneous detectors in the Monte Carlo calculations of Figs. 1a and b, we deduced the proportionality factor of 1.15. This correction factor was applied to the results from FLUKA82 and CASIM obtained by sampling the pion-induced showers in a homogeneous block of iron. The renormalization of the numerical results to minimum ionizing particles finally allows a direct test against the data of Ref. [11] for pion momenta of 40 and 86 GeV/c, respectively.
As seen from Figs. 3a and b the longitudinal energy deposition at both pion energies is generally reproduced by the codes within 50 % accuracy, the largest deviations are observed in the first two readout planes and particularly for the CASIM code in the tail of the distribution (up to a factor of 5).
The lateral energy deposition in the third readout plane is shown in Figs. 4a and b for the two different pion momenta. All codes describe the general behaviour of the data well although the distribution obtained by CASIM is systematically narrower compared to the data as well as to the other calculations.

To summarize the discussion of this section we have found that the main characteristics of the data, such as energy dependence and other features of the three-dimensional shower development, are described by the Monte Carlo codes FLUKA82 and GHEISHA within a general uncertainty of about 50 %. Some systematic deviations seem to appear in the comparison to the data describing the lead calorimeter of Ref. [10], particularly with increasing lateral

distance from the beam axis. The approximate treatment of the electromagnetic shower components in FLUKA82 is sufficient for the description of average shower properties, reducing the CPU-time requirements as compared to GHEISHA by at least one order of magnitude for energies above 100 GeV.
By using weighting techniques for both hadronic and electromagnetic shower components CASIM is faster by a factor of 20 to 50 compared to FLUKA82 in the considered energy range. However, there are systematic deviations from data up to a factor of 5. For these reasons we mainly rely on FLUKA82 and GHEISHA results in the next section.

## 4. Applications towards the design of the HERA Beam Dump

There are several typical problems which are important for the layout of beam abort systems at high-energy machines, including estimates of the maximum energy density to be expected near the axis of the incident beam as well as shielding requirements to protect, for example, superconducting magnets. Particularly for an internal dump like that planned for HERA there is also the question whether some extra shielding is necessary against particles escaping from the dump in forward directions through the beam pipe. All these problems represent rather extreme situations for routine calculations with Monte Carlo codes, therefore the corresponding numerical results are expected to be sensitive to details of the physical models used by the codes.

We start with the predictions for the energy density in the heat core around the beam axis. We have calculated the energy deposited by protons of 40 and 1000 GeV in different materials (carbon, aluminum, and copper) near the beam axis. Using a pointlike beam we extrapolated to realistic beam dimensions by looking for the energy density within a cylinder of 1 mm diameter (at the entrance of the dump the nominal beam size is $\sigma_h \simeq 0.5$ mm, $\sigma_v \simeq 0.8$ mm). In Figs. 5a–c we show the material dependence of the energy densities in the core ($r \leq 0.5$ mm) for protons of 1000 GeV versus the depth in different materials. For a discussion of the sizable differences between the predictions of GHEISHA and FLUKA82 we give magnitudes and positions of the maxima together with the ionization losses expected from incident protons in Table 1. For comparison the energy densities to reach the melting temperatures are also given. For protons of 40 GeV the maximum is observed within the first 5 cm of the target. The results from GHEISHA are 15 % higher for Al and C, and 40 % higher for Cu than pure ionization losses. Additional contributions from ionization losses of secondaries and nuclear excitation remaining after inelastic hadron-nucleus interactions raise the maximum obtained by FLUKA82 by a factor of 2 for Al and C, and a factor of 3 for Cu. If we consider carbon (density $\rho = 1.71$ gcm$^{-3}$) with a nuclear interaction length of 50 cm, about 10 % of the incident protons interact within the first 5 cm of the target, so that the energy deposition is expected to exceed the primary ionization losses. FLUKA82 with its assumptions on the interaction process (one third of the phenomenologically parametrized nuclear excitation energy is deposited locally at the interaction point) and a threshold energy $E_{thr} = 50$ MeV (particles below $E_{thr}$ are stopped locally) could result in some overestimate.
The deviations between FLUKA82 and GHEISHA are particularly evident for 1000 GeV protons incident on a carbon target. Fig. 6 shows the most important contributions to the energy deposition in carbon obtained by FLUKA82; the energy deposition has been averaged within a cylinder of 1 mm diameter around the pointlike beam as in the previous cases. Due to the high multiplicities of secondaries generated at very small angles, the ionization losses



of these secondaries govern the maximum of the energy deposition in this material. We expect the increase of the contribution from electromagnetic showers to be too slow because of the parametrization used by FLUKA82: The lateral shower dimension reflects the average behaviour, e.g. it is independent of longitudinal shower development, resulting in a too broad energy distribution at the beginning of the shower.
As can be seen from Table 1 and Fig. 5, the energy deposition changes considerably for 1000 GeV protons when going from carbon to copper. The longitudinal and lateral development of electromagnetic cascades is governed by the hadronic absorption length $\lambda$, the radiation length $X_0$, and the Molière radius $\rho_M$ given in Table 2. The strong material dependence of these quantities results in a maximum energy density in copper that is dominated by electromagnetic showers, while this contribution to the maximum energy density in carbon is completely negligible against the ionization losses of charged secondaries (Fig. 6). This explains the strong increase in the value of the maximum from carbon to copper at 1000 GeV found in Table 1.
The application of the codes to incident protons of 1000 GeV increases the uncertainties of the underlying physical models, particularly those inherent in the description of particle production processes (e.g., muliplicities and energy spectra of secondaries). To study the influence of those extrapolations further we compare results from FLUKA82 and GHEISHA for the energy density in three different lateral bins of a carbon target to the predictions of the CASIM and MARS programs [**12,13**] in Fig. 7. The beam size is defined as in Ref. [**12**]. The GHEISHA results are in reasonable agreement with the MARS results although they are somewhat higher for larger radii within the first 50 cm of carbon. For FLUKA82 the energy deposition rises faster at small depth and is smaller at larger depth.
The laterally integrated longitudinal energy densities obtained by FLUKA82 and GHEISHA again agree within the accuracy found in the previous chapter. This demonstrates the importance of details in the description of energy deposition mechanisms for this particular application of the codes. As one can see from Table 1 carbon is the only material where the energy density for 1000 GeV protons does not reach the melting limit, but more detailed calculations on mechanical stresses due to the temperature rise have to demonstrate that graphite is a suitable material for the first part of a composite absorber block. This will be dealt with in a forthcoming report.
From the foregoing discussion we conclude that the predictions of different Monte Carlo codes for the target heating near the beam axis have a general uncertainty of a factor 2 to 3 at energies around 1000 GeV.

Next we estimated how much energy might be deposited in superconducting magnets due to particles escaping from the dump in forward directions. The superconducting coils of the magnets have been simulated by a 10 cm thick copper plate, installed at a distance $z$ behind the beam dump (see Fig. 8). Because of considerable statistical fluctuations we have averaged the energy density within the copper plate over the area of the beam pipe ($6 \times 6$ cm$^2$), where most of the escaping particles deposit their energy for geometrical reasons. The energy density versus the distance of the copper plate from the dump is given in Fig. 9; we assumed that $2 \cdot 10^{13}$ protons enter the dump. Since a considerable part of that energy is deposited by low-energy photons and electrons, the applicability of FLUKA82 to this problem is questionable because of the simplified treatment of the electromagnetic cascades in this code (compare section 2). Nevertheless the results of GHEISHA (with its sampling of electromagnetic cascades by EGS) and FLUKA82 agree within a factor of 2 to 5.

The first superconducting magnet of HERA will be located 80 m downstream of the absorber block. This type of magnet is expected to become normal conducting if a fast energy deposition exceeds a value of about 1 $mJg^{-1}$ (quench limit) [14]. Extrapolating the calculated energy deposition from Fig. 9, by means of an $r^{-2}$ behaviour, we estimate for a distance of 80 m behind the dump an energy deposition of 0.2 $mJg^{-1}$. This value is reduced by a factor of 2 because only neutrals have to be taken into account. Charged particles will be scattered into the beam pipe due to the quadrupole magnets right after the dump. The energy deposition is additionally reduced by at least a factor of 10 because the beam will be swept steadily downwards by 6 cm across the surface of the absorber block which enlarges the distance between the shower maximum and the beam pipe. Therefore the deposited energy is at least two orders of magnitude below the quench limit.

Finally we looked at the effect, on superconductors on the HERA tunnel walls, of particles escaping at wide angles from the dump. The superconductor was simulated by a 1 cm thick copper cylinder surrounding the dump at a distance of 2 m from the axis. The beam dump itself was represented by a carbon cylinder ($R$ = 10 cm) with a 15 cm thick iron cover (Fig. 10). As in the previous case the FLUKA82 results are significantly higher than the GHEISHA results, although the longitudinal shapes agree with each other as can be seen from Fig. 11. This could be due to differences in the treatment of intranuclear cascade nucleons, mainly neutrons, from inelastic hadron-nucleus collisions by both codes. In earlier applications of FLUKA82 this component has been found to dominate the particle fluxes at large angles to the beam [15].
Also in this case the deposited energy for $2 \times 10^{13}$ protons in the dump should not harm the superconductor. Even in case of a quench the superconductor could not be damaged: The conductor would be reinforced by thick copper bars soldered to it and the current would be switched off immediately after the dumping. Actually there are no superconductors foreseen at the HERA tunnel walls next to the beam dump at all.

## 5. Summary

In this paper we have used different Monte Carlo codes for the simulation of hadron-induced showers installed at DESY—GHEISHA 7.3, FLUKA82, and CASIM. A comparison of calculated three-dimensional energy depositions with data taken at primary energies up to 300 GeV shows that the main features of the experimental results are reproduced by the FLUKA82 and GHEISHA codes usually within a 50 % accuracy. This is true for various types of incident particles (protons and pions), various primary energies, and various materials, although there are some systematic differences between the numerical results and the data from the lead calorimeter [10], particularly for larger distances from the beam axis. CASIM cannot describe several characteristics of the three-dimensional shower development: Especially the tail of the longitudinal distributions as well as the slow increase towards the shower maximum and its position at larger distances from the beam axis ($\geq$ 4 cm for iron) show considerable deviations from the data and from the other Monte Carlo results.
The application of GHEISHA and FLUKA82 to the study of shielding problems around the HERA beam dump confronts both programs with rather extreme situations. The Monte Carlo results are expected to depend strongly on special details of the shower development such as the description of the electromagnetic shower component and the intranuclear cascade processes in inelastic hadron collisions. Corresponding differences between the codes show



up in deviations reaching up to a factor of 5 in particular situations.
Taking these uncertainties into account one can conclude that for $2 \times 10^{13}$ protons, dumped into a 7 m long absorber block with 50 cm diameter composed of C, Al, and Cu, no superconductor will become normal conducting. Furthermore, the temperatures stay an order of magnitude below melting temperatures if the beam is swept steadily through 6 cm across the front face of the dump during the dumping.

ACKNOWLEDGEMENTS

We are much obliged to Dr. D. Lüke for his help and effort in installing the programs on the IBM 3081 in Düsseldorf mainly used for our calculations. Without this support our work would not have been possible.
One of us (H.-J. Möhring) would like to thank the DESY Directorate for offering and supporting this work on HERA problems, as well as his colleagues for the interesting collaboration.

## REFERENCES


1. W. R. Nelson and T. M. Jenkins (Eds.), *Computer Techniques in Radiation Transport and Dosimetry*, plenum press, New York (1980).

2. H. Fesefeldt, Preprint TH Aachen PITHA-85-02 (1985).

3. P. A. Aarnio, J. Ranft, G. R. Stevenson, *A long write up of the FLUKA82 program*, CERN Divisional Report TIS-RP/106 (June 1983); and TIS-RP/129 (April 1984).

4. A. Van Ginneken, *CASIM. Program to Simulate Hadronic Cascades in Bulk Matter*, Fermilab Report FN-272 (1975); *Calculation of the Average Properties of Hadronic Cascades at High Energies (CASIM)*, see Ref. 1, lecture 21, p. 323.

5. R. L. Ford and W. R. Nelson, *The EGS Code System (Version 3)*, SLAC Report SLAC-210 (1978).

6. J. Ranft and J.Routti, Comp. Phys. Comm **7** (1974), p. 327.

7. K. Häußgen, H. - J. Möhring and J. Ranft, Nucl. Sci. Eng. **88** (1984), p. 551; K. Häußgen and J. Ranft, Nucl. Sci. Eng. **88** (1984), p. 537; J. Ranft and S. Ritter, Z. Phys **C20** (1983), p. 347;
J. Ranft and S.Ritter, *The MC codes NUCENT and HADENT to Simulate Hadron Production in Hadron-Nucleus and Hadron-Hadron Collisions*, CERN Internal Report TIS/IR/83-23 (1983).

8. P. Aurenche, F. W. Bopp and J. Ranft, Z. Phys **C23** (1984), p. 67.

9. R. Hagedorn, Suppl. Nuovo Cim. **3** (1965), p. 147; R. Hagedorn and J. Ranft, Suppl. Nuovo Cim. **6** (1968), p. 169; H. Grote, R. Hagedorn and J. Ranft, *Atlas of Particle Spectra*, CERN, Geneva, Switzerland (1970).

10. Y. Muraki et al., Nucl. Instr. Meth. **A236** (1985), p. 47.

11. D. Bollini et al., Nucl. Instr. Meth. **171** (1980), p. 237.

12. N. V. Mokhov, *Energy deposition in targets and beam dumps at 0.1-5 TeV proton energy*. Fermilab Report FN-328 (1980).

13. A. N. Kalinovsky, N. V. Mokhov and Yu. P. Nikitin, *Penetration of High Energy Particles Through Matter*. Energoatoimizdat, Moscow, USSR (1984); N. V. Mokhov, IHEP Preprint 82-168, Serpukhov, USSR (1982).

14. B. Cox, P.O. Mazur, A. Van Ginneken, IEEE **NS-26** (1979), p. 3885.

15. H.-J. Möhring and J. Ranft, Nucl. Sci. Eng. **89** (1985), p. 247; G.R.Stevenson et al., Nucl. Instr. Meth. **A245** (1986), p. 323.




## TABLES

| | $z$-position of maximum (cm) | | $\varepsilon$ (kJ/g) | | $E_m = c \cdot t_m$ (kJ/g) | $dE/dx$ (kJ/g) |
|---|---|---|---|---|---|---|
| | FLUKA82 | GHEISHA | FLUKA82 | GHEISHA | | |
| 40 GeV | | | | | | |
| C | 0 - 5 | 0 - 5 | 1.5 | 0.77 | 6.80 | 0.67 |
| Al | 0 - 5 | 0 - 5 | 1.5 | 0.74 | 0.59 | 0.64 |
| Cu | 0 - 5 | 0 - 5 | 1.8 | 0.80 | 0.42 | 0.58 |
| 1000 GeV | | | | | | |
| C | 5 - 20 | 100 - 125 | 3.8 | 2.0 | 6.80 | 0.67 |
| Al | 20 - 25 | 40 - 65 | 4.2 | 4.2 | 0.59 | 0.67 |
| Cu | 15 - 20 | 12.5 - 17.5 | 28.0 | 22.0 | 0.42 | 0.61 |

**Table 1** : Magnitude and position of maximum energy density $\varepsilon$ ($\mathrm{kJg}^{-1}$) obtained by the GHEISHA and FLUKA82 Monte Carlo codes. (Pointlike proton beam, cross section area of the heat core $R$ = 0.5 mm.)

| material | $\lambda$ (cm) | $X_0$ (cm) | $\rho_M$ (cm) |
|---|---|---|---|
| C | 50.5 | 25.0 | 5.73 |
| Al | 39.4 | 8.89 | 4.41 |
| Cu | 15.1 | 1.43 | 1.58 |

**Table 2** : Material dependence of hadronic absorption length $\lambda$, radiation length $X_0$, and Molière radius $\rho_M$.

## FIGURE CAPTIONS

**Fig. 1 :** Comparison of energy densities obtained by different Monte Carlo codes, with data [**10**]. A 300 GeV/c proton beam is incident on: -
a) an iron calorimeter
b) a lead calorimeter
The longitudinal development of the energy densities for three different radial distances r from the shower axis is shown.

**Fig. 2 :** Average longitudinal energy deposition for hadronic showers induced by 86 GeV/c pions in an iron calorimeter, calculated by the GHEISHA-code for two different models: -
- Simulation of readout planes by 7 mm scintillator material (full line)
- Readout plane simulated by 1 mm iron plates (dashed line).

**Fig. 3 :** Laterally integrated longitudinal energy deposition in the iron calorimeter of Ref. [**11**] compared to Monte Carlo results for incident pion momenta of: -
a) 40 GeV/c
b) 86 GeV/c
(Note that the results from FLUKA82 and CASIM have been renormalised by a factor of 1.15 obtained from Fig. 2.)

**Fig. 4 :** Lateral energy deposition in the third readout plane of the same calorimeter as in Fig. 3 for: -
a) 40 GeV/c
b) 86 GeV/c

**Fig. 5 :** Energy densities obtained within a cylinder of 1 mm of diameter for a 1000 GeV/c pointlike proton beam in different materials: -
a) carbon
b) aluminum
c) copper

**Fig. 6 :** Contributions of different mechanisms to the energy density in a carbon target within a cylinder of 1 mm diameter around a pointlike 1000 GeV proton beam: -
(1) ionization losses of secondary hadrons
(2) local nuclear excitation energy
(3) electromagnetic showers
(4) ionization from primary protons
(5) total energy density
The curves have been obtained with FLUKA82.



**Fig. 7 :** Energy density $\varepsilon$ versus depth $z$ in different radial bins caused by a 1000 GeV proton beam incident on a carbon target ($\rho$ = 1.71 gcm$^{-3}$). The range of predictions obtained from different versions of CASIM and MARS [**12**,**13**] programs is represented by the hatched area. The gaussian beam size is the same as in Ref. [**12**]: $\sigma_v$ = 0.07 cm, $\sigma_h$ = 0.14 cm.

**Fig. 8 :** Simulation of the HERA beam dump, used to estimate the influence, on downstream superconducting magnets, of particles escaping through the beam pipe. The cross shown in the front view marks the initial entry point of the beam. During the dump process the beam will be swept steadily downwards by 6 cm.

**Fig. 9 :** Energy deposition in a copper plate behind the beam dump, averaged over the area of the beampipe, versus the distance from the dump. (Pointlike 1000 GeV/c proton beam incident on the dump as shown in Fig. 8, $2 \times 10^{13}$ protons.)

**Fig.10 :** Simulation for studying the radial shielding of the proton beam dump.

**Fig.11 :** Energy deposition in a copper cylinder of thickness 1 cm surrounding the beam dump (see Fig. 10) for $2 \times 10^{13}$ incident protons with momentum of 1000 GeV/c.

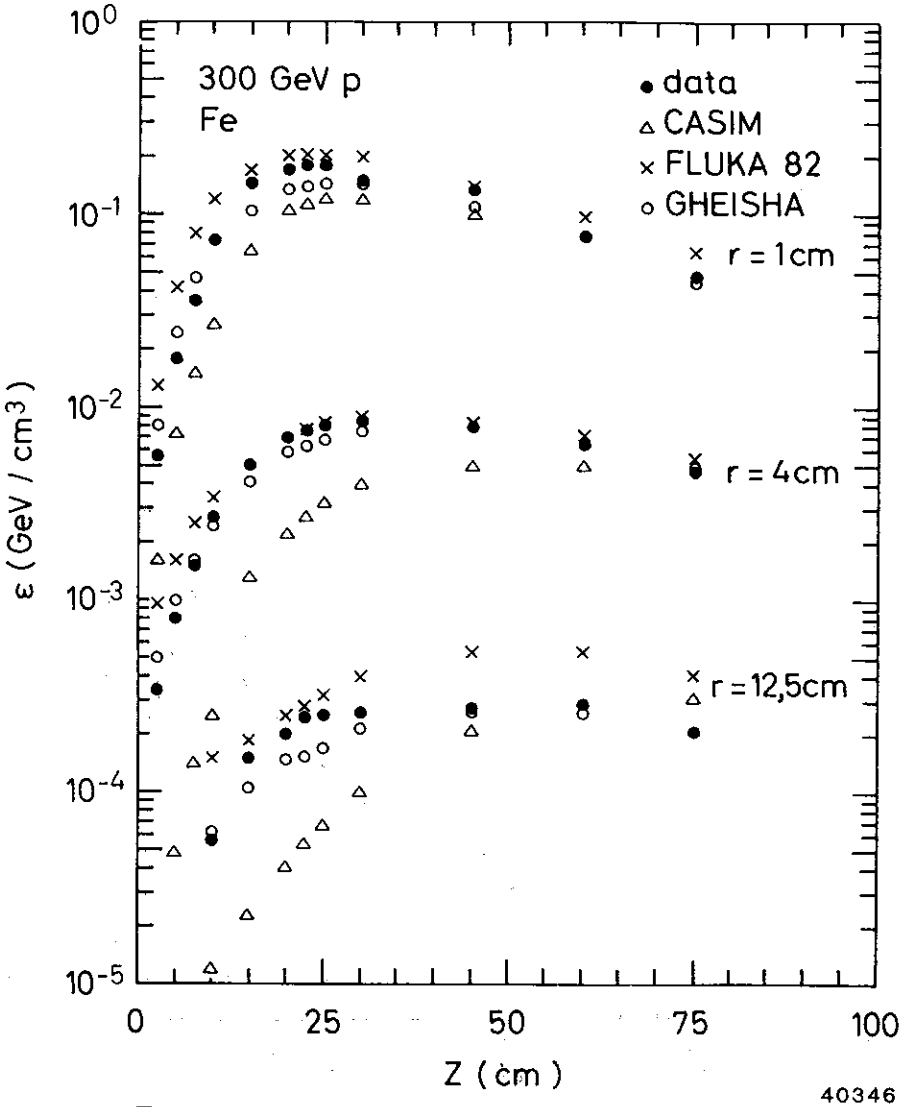
300 GeV p
Fe
data
CASIM
FLUKA 82
GHEISHA
r = 1cm
r = 4cm
r = 12,5cm
ε ( GeV / cm³ )
Z ( cm )
40346

Fig. 1a

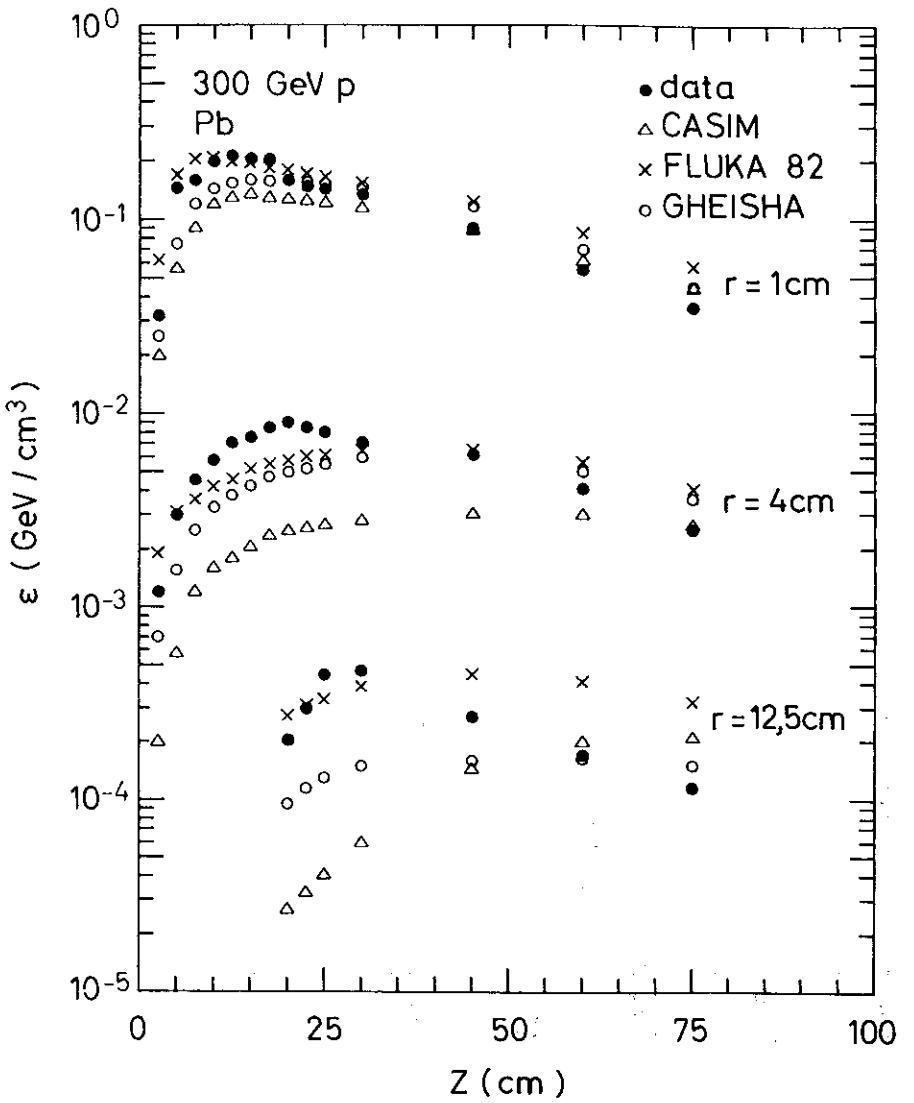
300 GeV p
Pb
data
CASIM
FLUKA 82
GHEISHA
r = 1cm
r = 4cm
r = 12,5cm
ε ( GeV / cm³ )
Z ( cm )
40345

Fig. 1b

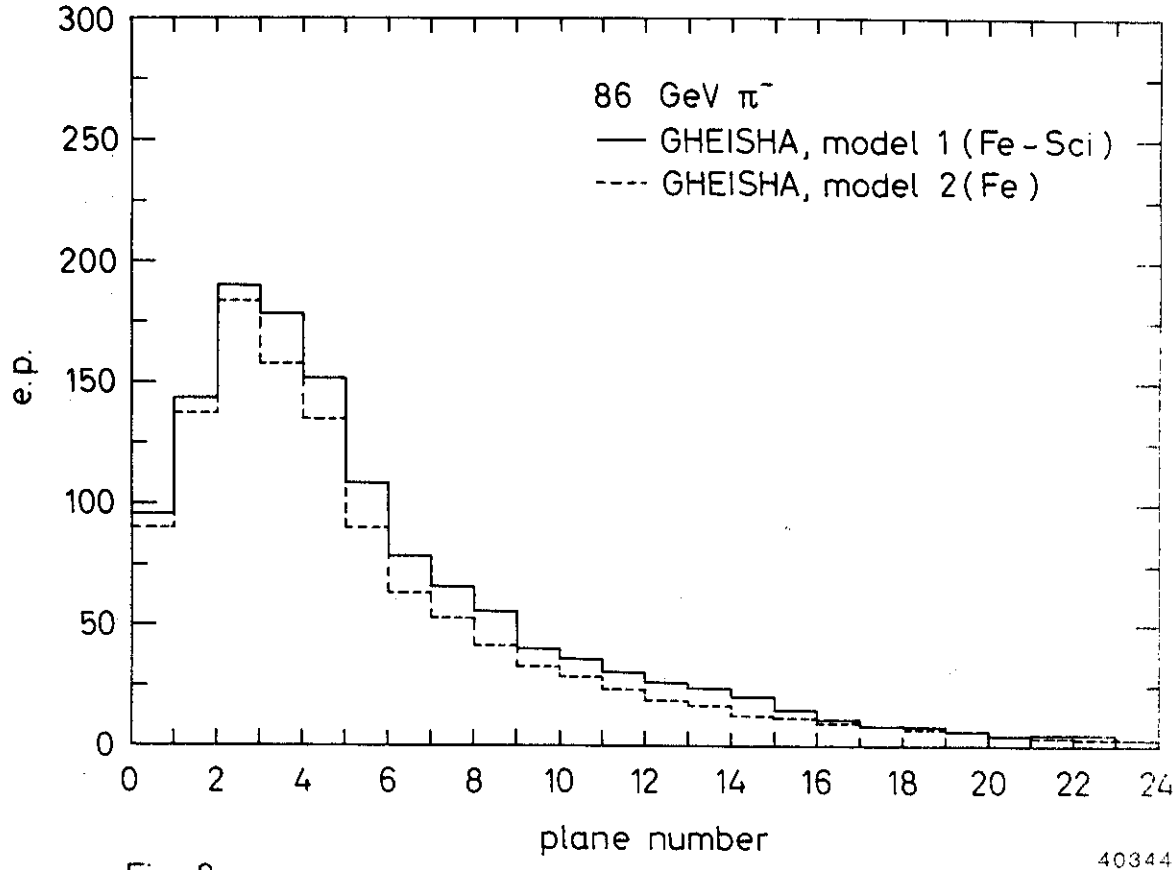
86 GeV π⁻
GHEISHA, model 1 (Fe-Sci)
GHEISHA, model 2 (Fe)
e.p.
plane number
0
50
100
150
200
250
300
0 2 4 6 8 10 12 14 16 18 20 22 24
40344

Fig. 2

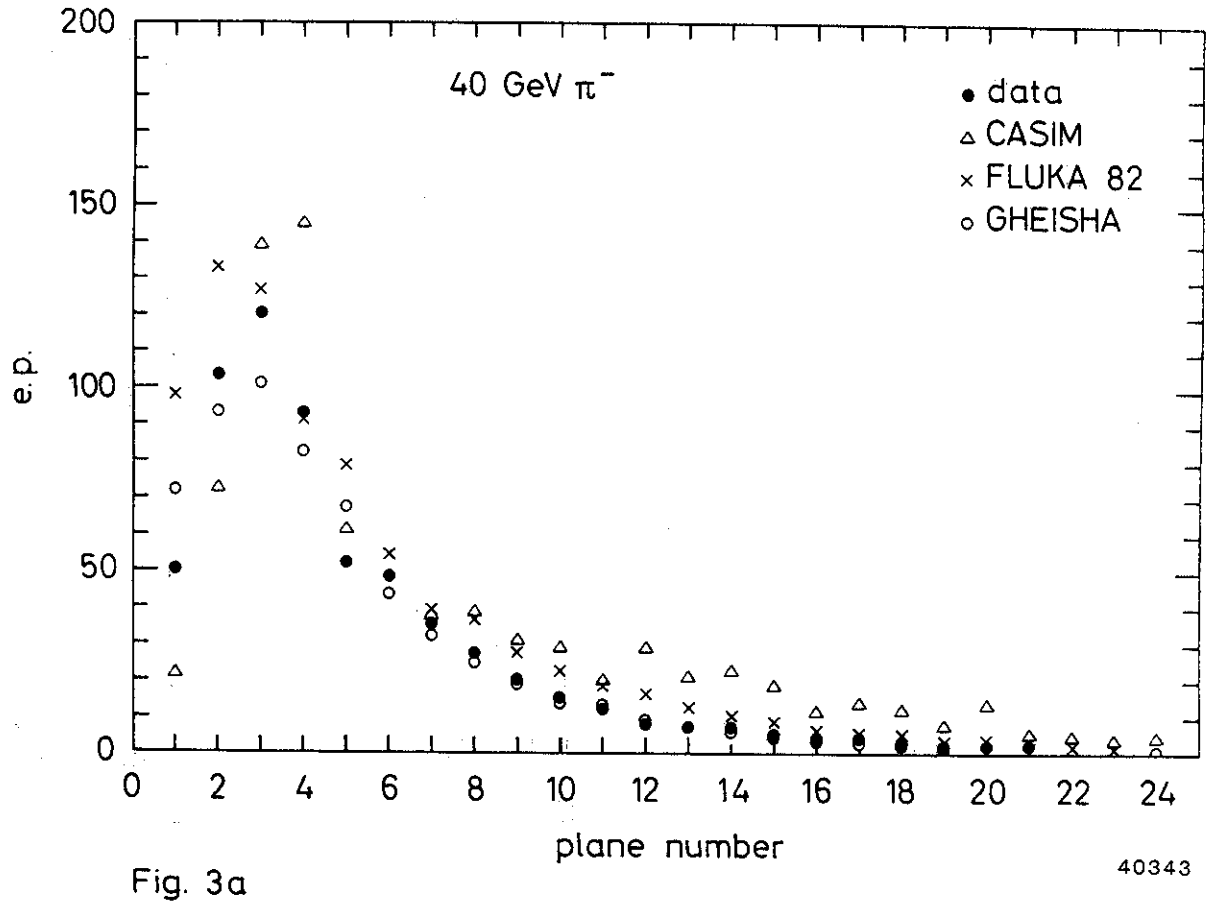
40 GeV π⁻
data
CASIM
FLUKA 82
GHEISHA
e.p.
plane number
0
50
100
150
200
0 2 4 6 8 10 12 14 16 18 20 22 24
40343

Fig. 3a

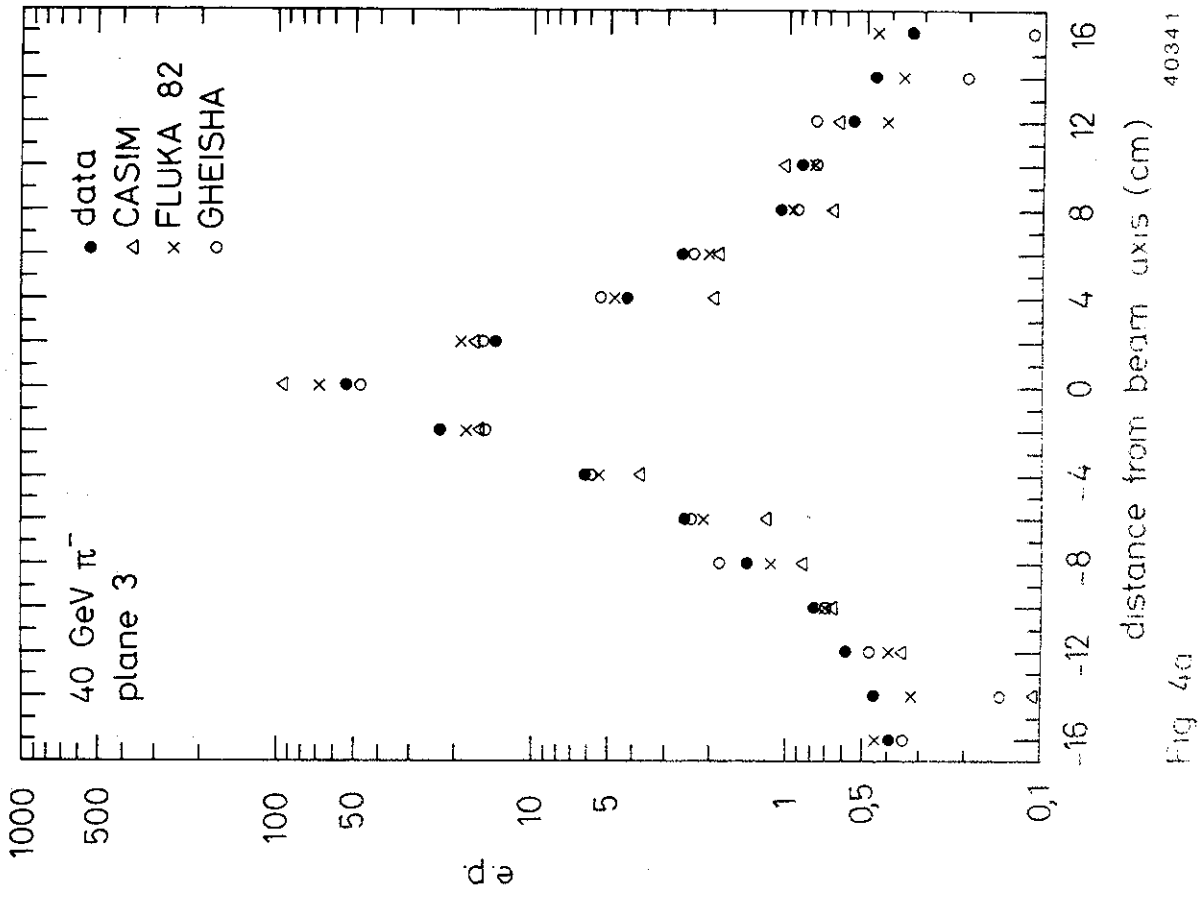
data
CASIM
FLUKA 82
GHEISHA
40 GeV π⁻
plane 3
e.p.
1000
500
100
50
10
5
1
0,5
0,1
-16
-12
-8
-4
0
4
8
12
16
distance from beam axis (cm)
40341

Fig 4a

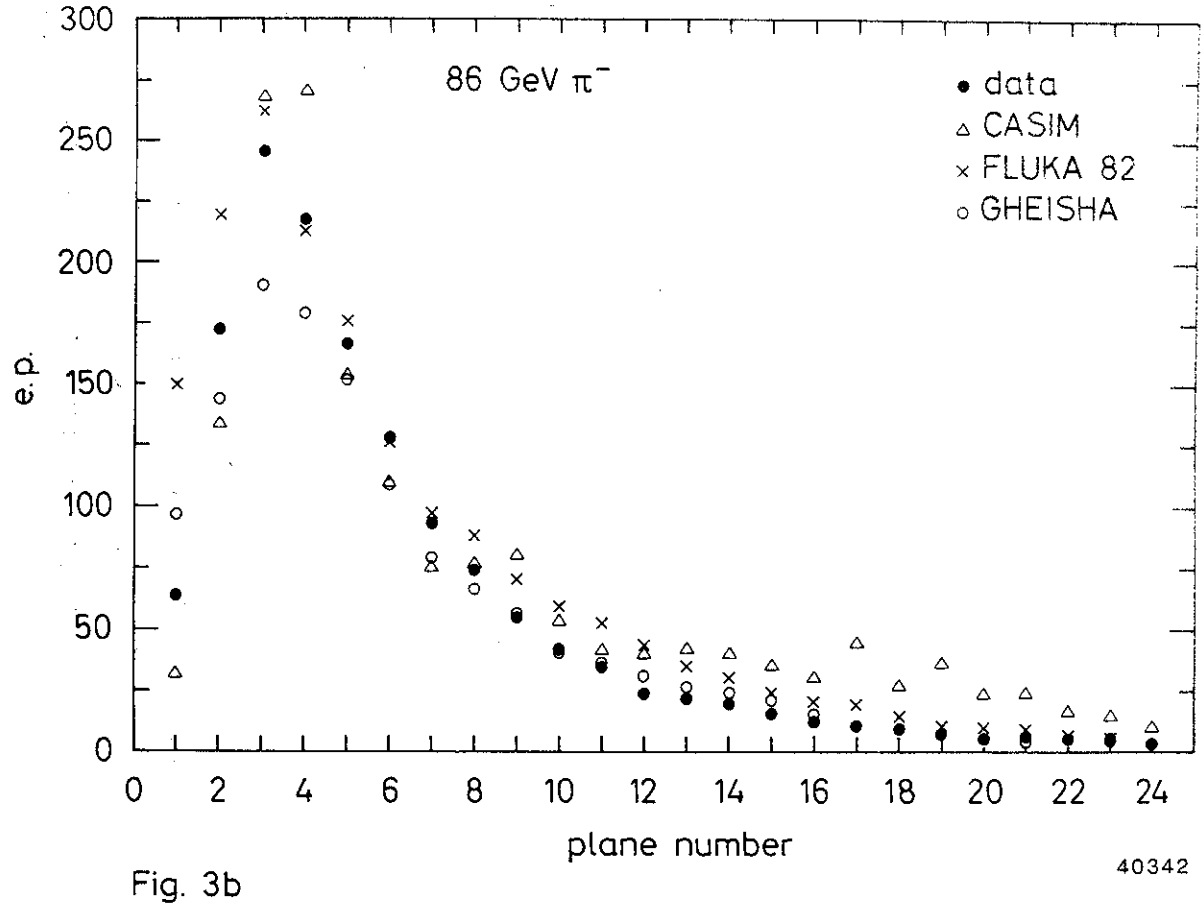
86 GeV π⁻
data
CASIM
FLUKA 82
GHEISHA
e.p.
300
250
200
150
100
50
0
0
2
4
6
8
10
12
14
16
18
20
22
24
plane number
40342

Fig. 3b

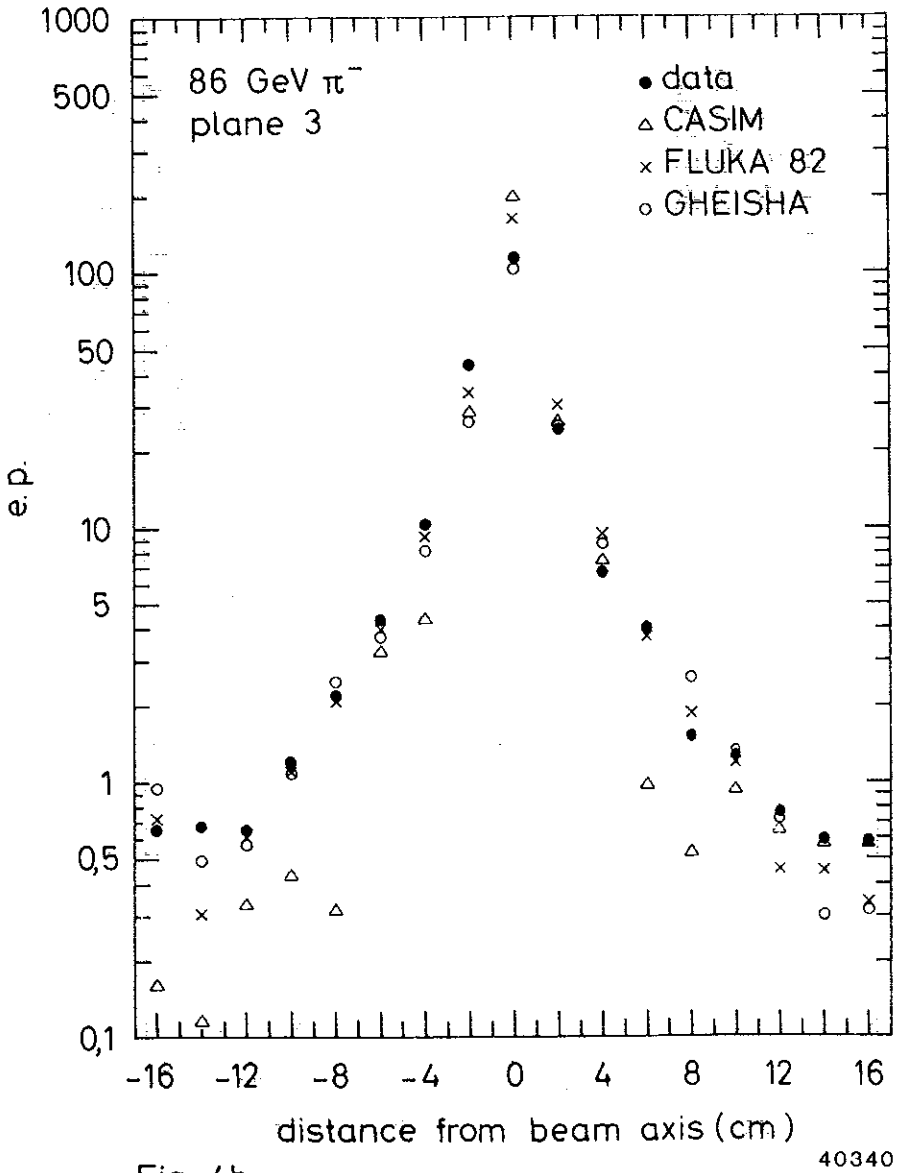
86 GeV π⁻
plane 3
● data
△ CASIM
× FLUKA 82
○ GHEISHA
e.p.
1000
500
100
50
10
5
1
0,5
0,1
-16
-12
-8
-4
0
4
8
12
16
distance from beam axis (cm)
40340

Fig. 4b

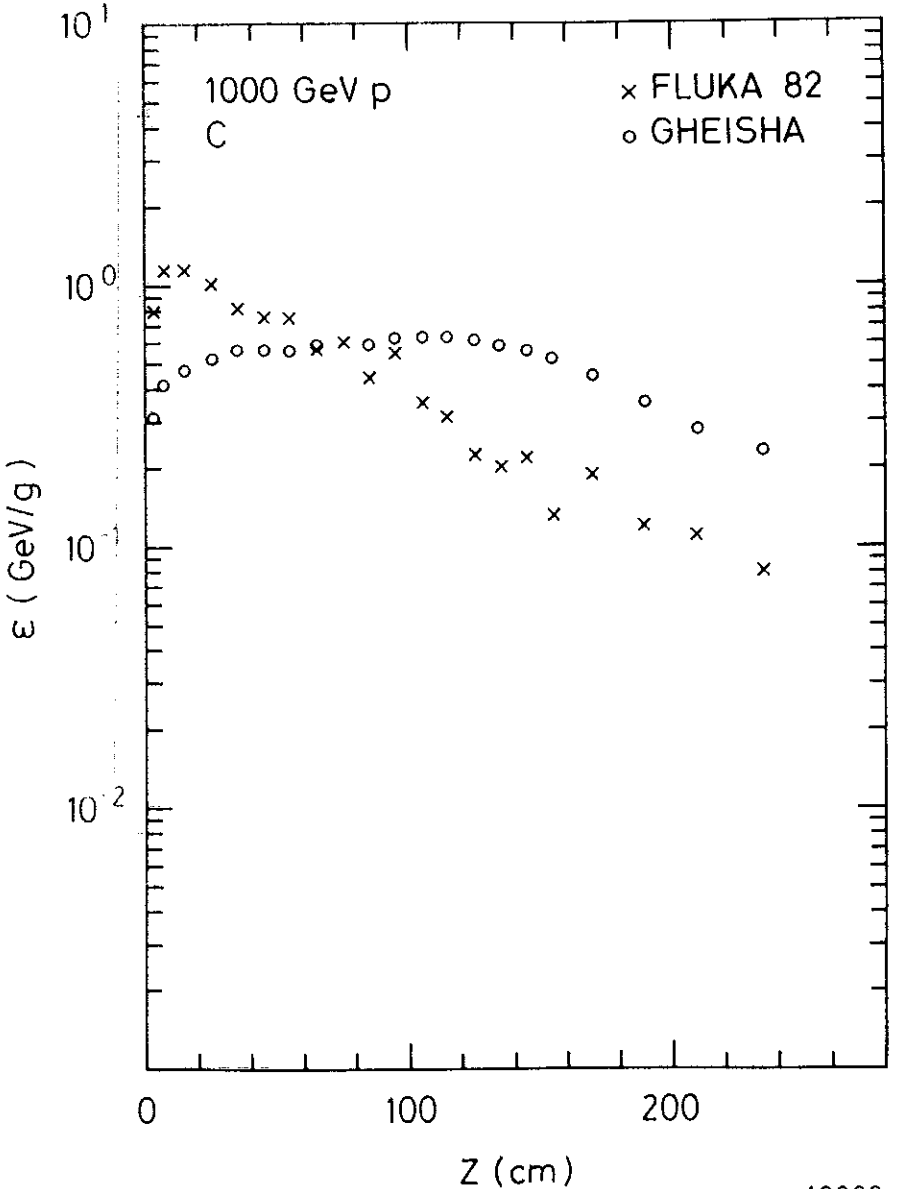
1000 GeV p
C
× FLUKA 82
○ GHEISHA
ε ( GeV/g )
10¹
10⁰
10⁻¹
10⁻²
0
100
200
Z (cm)
40339

Fig. 5a

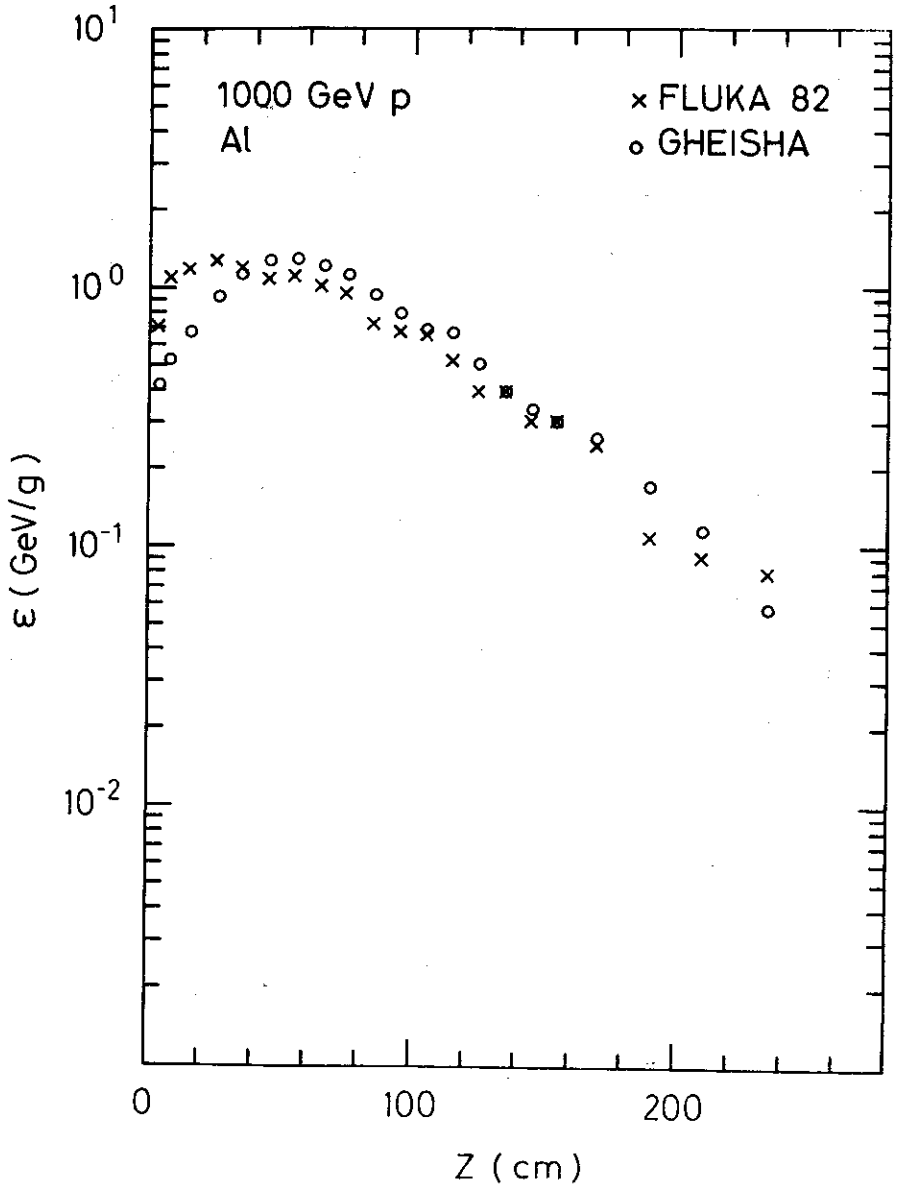


Fig. 5b

40338

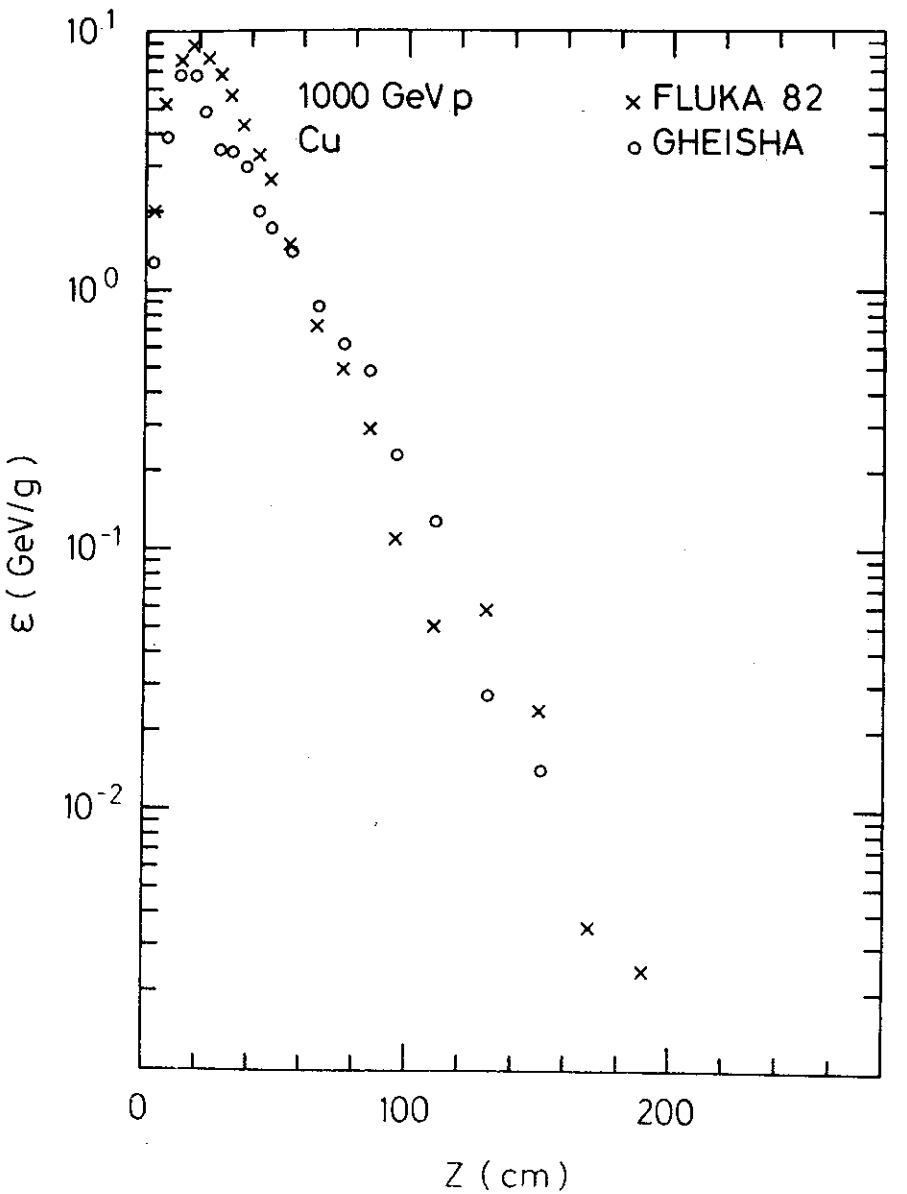


Fig. 5c

40337

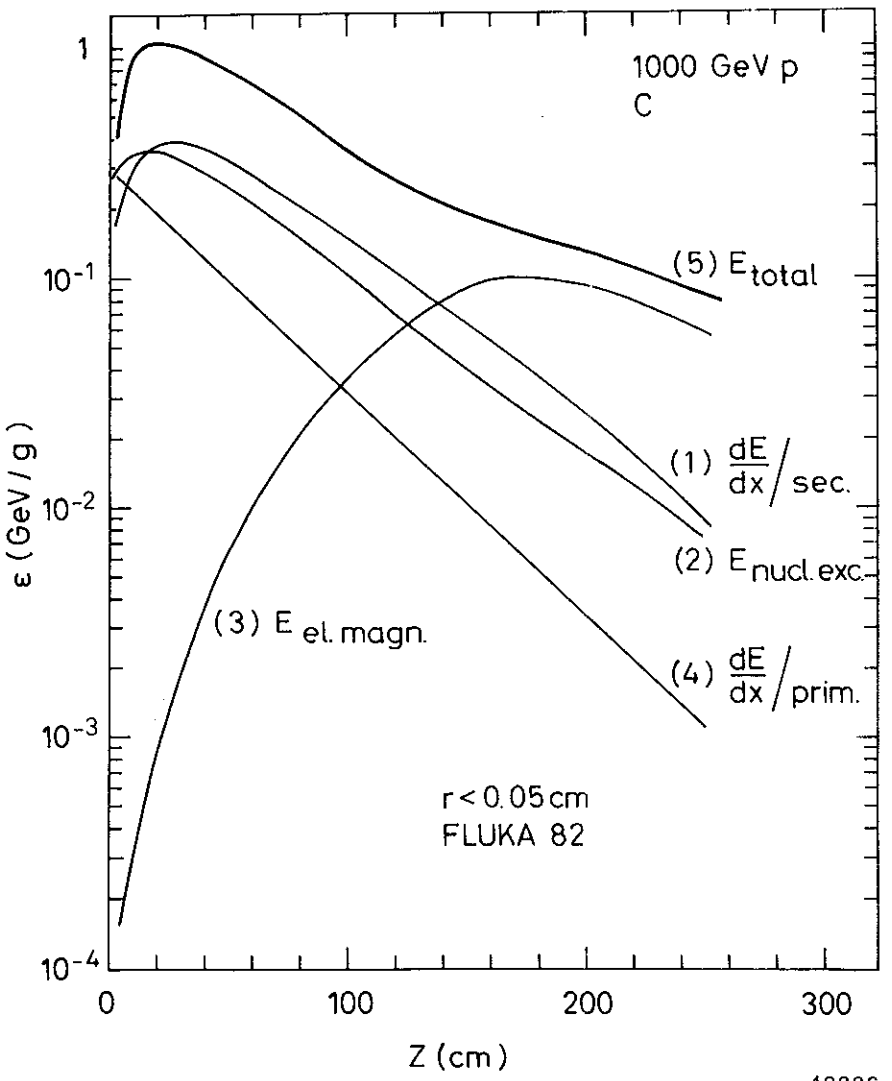
1000 GeV p
C
(5) E total
(1) dE/dx sec.
(2) E nucl. exc.
(3) E el. magn.
(4) dE/dx prim.
r < 0.05 cm
FLUKA 82
ε (GeV/g)
Z (cm)
40336

Fig. 6

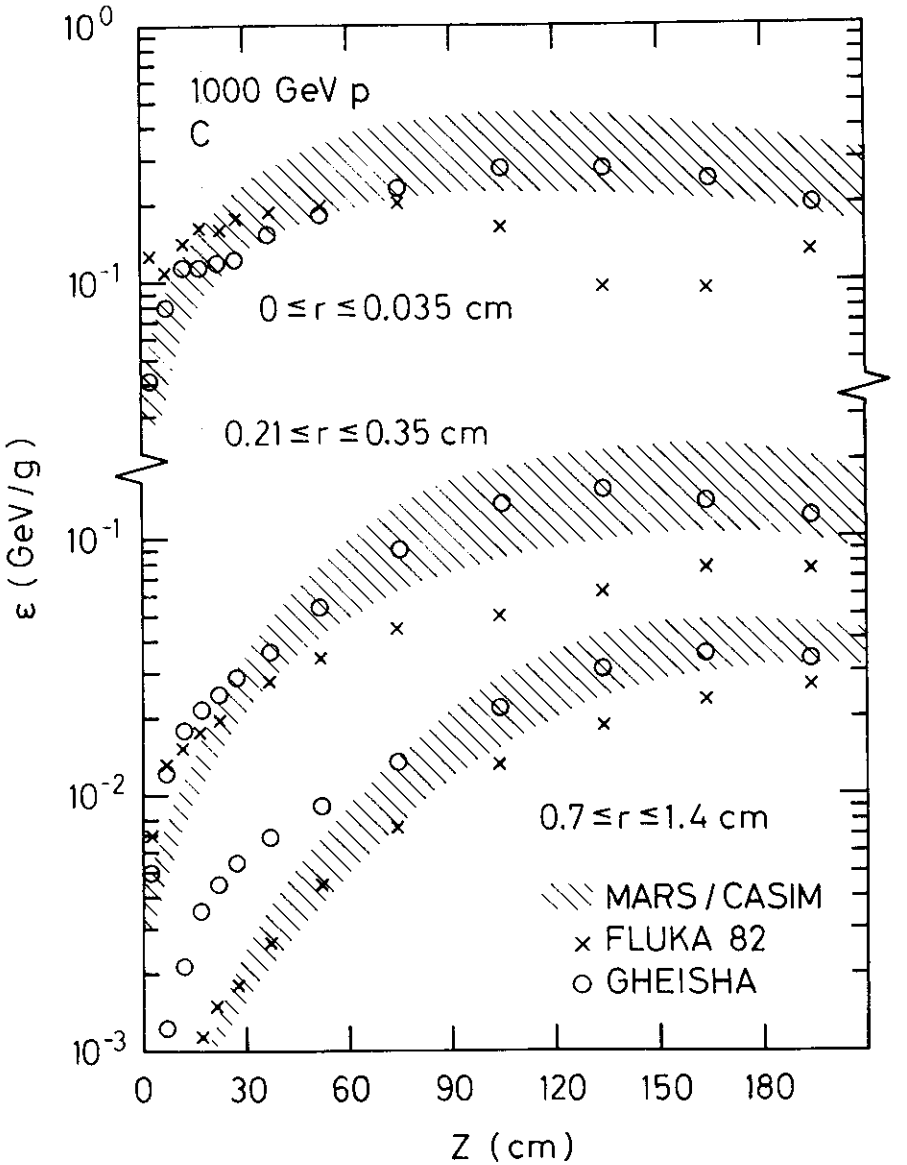
1000 GeV p
C
0 ≤ r ≤ 0.035 cm
0.21 ≤ r ≤ 0.35 cm
0.7 ≤ r ≤ 1.4 cm
MARS / CASIM
× FLUKA 82
○ GHEISHA
ε (GeV/g)
Z (cm)
40335

Fig. 7

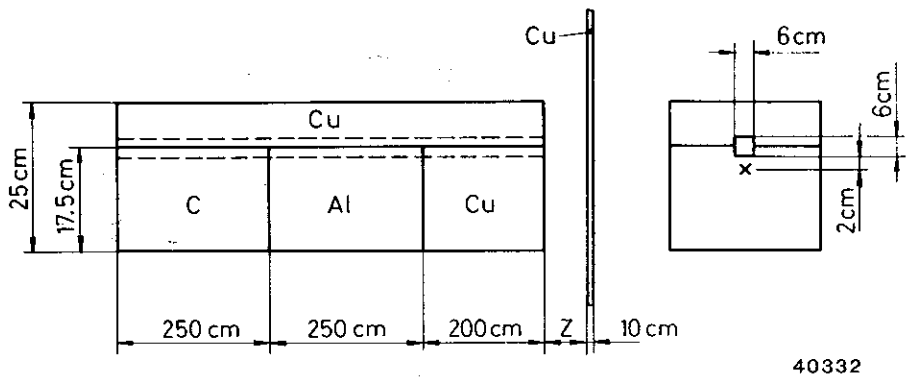
Cu
6cm
Cu
6cm
25cm
17.5cm
C
Al
Cu
2cm
250 cm
250 cm
200cm
Z
10 cm
40332

Fig. 8

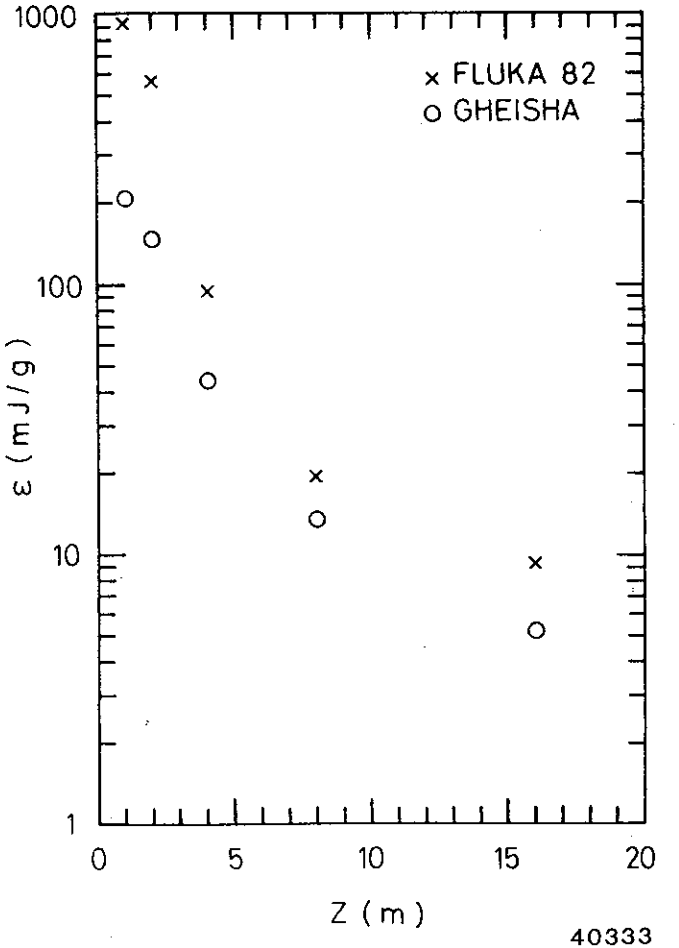
1000
100
10
1
ε ( mJ/g )
× FLUKA 82
o GHEISHA
0
5
10
15
20
Z ( m )
40333

Fig. 9

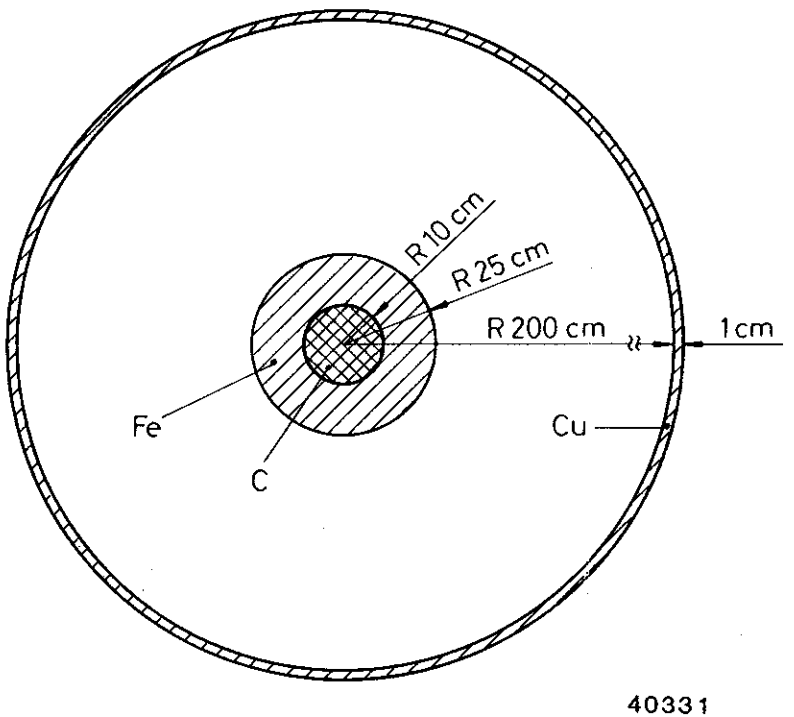
R 10 cm
R 25 cm
R 200 cm
1 cm
Fe
C
Cu
40331

Fig. 10

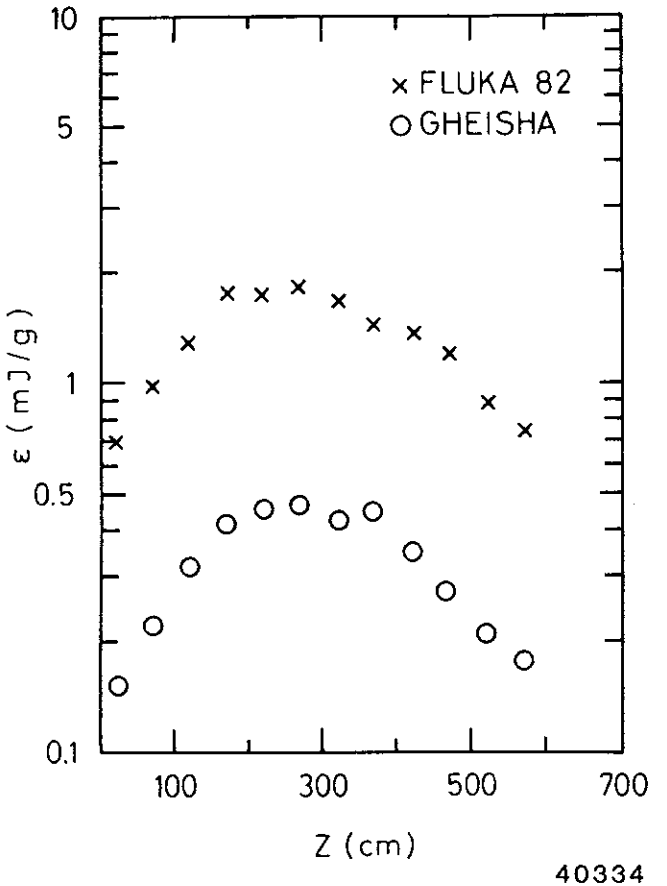
10
5
1
0.5
0.1
ε (mJ/g)
× FLUKA 82
○ GHEISHA
100
300
500
700
Z (cm)
40334

Fig. 11